^{1}H-NMR of $Rh(NH_3)_4phi^{3+}$ Bound to $d(TGGCCA)_2$: Classical Intercalation by a Nonclassical Octahedral Metallointercalator

J. Grant Collins,† Thomas P. Shields, and Jacqueline K. Barton*

Contribution from the Division of Chemistry and Chemical Engineering, Beckman Institute, California Institute of Technology, Pasadena, California 91125

Received January 4, 1994®

Abstract: ^{1}H-NMR studies of $Rh(NH_3)_4phi^{3+}$ (phi = 9,10-phenanthrenequinone diimine) bound to $d(TGGCCA)_2$ indicate that the octahedral complex binds to the duplex in a manner consistent with classical intercalation. Upfield shifts of the phi protons of $Rh(NH_3)_4phi^{3+}$ upon binding to the oligonucleotide are observed with the greatest shift seen for the (2,7) protons followed by (1,8) > (3,6) ~ (4,5). From the chemical shift differences of the inequivalent phi (2,7) proton resonances (determined at 285 K) the exchange rate is estimated to be approximately 250 s^{-1} at the coalescence temperature of 305 K and ~10 s^{-1} at 285 K. The NOESY of the 1:1 $Rh(NH_3)_4phi^{3+}$–$d(TGGCCA)_2$ complex reveals a complete absence of an NOE cross peak between the C_4H6 and the $G_3H2'/H2''$ protons, and instead NOE cross peaks between phi protons and protons from the G_3 and C_4 residues are observed. The one- and two-dimensional NMR data are consistent with the rhodium complex intercalated into the G_3C_4 site from the major groove. Molecular modeling based on these data leads to a structure of $Rh(NH_3)_4phi^{3+}$ intercalated from the major groove with the phi ligand fully inserted and stacked in the column of base pairs. In this model the axial ammines of $Rh(NH_3)_4phi^{3+}$ are well positioned for hydrogen bonding to the guanine O6 atoms. A comparison of this NMR study to those with Δ-$Ru(phen)_3^{2+}$ and Δ-$Rh(phen)_2phi^{3+}$ is made; the tetraammine complex appears to be intercalated more deeply in the intercalation pocket. In general, based upon these data, the DNA binding mode of $Rh(NH_3)_4phi^{3+}$ may be considered as classical intercalation. Octahedral metallointercalators, however, may be considered as nonclassical; their sequence-selectivity is derived from the nonintercalating functionalities of the synthetic, octahedral complex. These structural studies provide the basis for the design of sequence-specific DNA-binding complexes in the major groove.

Introduction

Coordinatively saturated, octahedral metal complexes offer versatile model systems to explore principles of nucleic acid recognition and a foundation for the design of novel DNA-targeted chemotherapeutics.[1-8] Metal complexes containing extended aromatic heterocyclic ligands have been shown to bind DNA noncovalently through intercalation in the major groove, where the heterocyclic ligand is inserted partially between the base pairs so as to maximize stacking interactions. The overall DNA binding affinity of these octahedral complexes has been found to correlate with the surface area for stacking of the heterocyclic ligand.[3,6,9] The site specificity of these metal complexes has been seen to result from both shape-selective steric interactions[1-3] as well as stabilizing van der Waals and hydrogen bonding contacts.[6,10] Intercalative binding therefore offers a strategy for the predictive design of new DNA binding complexes; a metal complex may be anchored in the DNA helix via intercalation of a bidentate aromatic ligand so that in three dimensions the four ancillary ligands become available for sequence-selective interaction in the major groove. Using this approach, metal complexes are being designed that bind to DNA with high affinity at specific sequences.[7,10]

So as to extend this strategy in a predictive fashion, there has been considerable interest in establishing the precise mode of association of these complexes with DNA. Additionally, some debate has arisen as to whether octahedral complexes can in fact bind through a classical intercalative mode or whether the structural details of such binding by a non-planar octahedral complex need refinement.[11-16] Hence we have undertaken a series of structural studies to characterize the intercalative binding of different octahedral complexes with double helical oligonucleotides.

Recently our laboratory has provided structural evidence via ^{1}H NMR for specific intercalation of Δ-$Rh(phen)_2phi^{3+}$ (phi =

* Author to whom correspondence should be addressed.
†Permanent address: Department of Chemistry, University College, University of New South Wales, Australian Defence Force Academy, Campbell, ACT, 2600, Australia.

® Abstract published in *Advance ACS Abstracts*, October 1, 1994.

(1) (a) Pyle, A. M.; Barton, J. K. *Prog. Inorg. Chem.* 1990, *38*, 413. (b) Chow, C. S.; Barton, J. K. *Methods Enzymol.* 1992, *212*, 219. (c) Barton, J. K. *Science* 1986, *233*, 727; (d) Murphy, C. J.; Barton, J. K. *Methods Enzymol.* 1993, *226* 576.

(2) (a) Pyle, A. M.; Long, E. C.; Barton, J. K. *J. Am. Chem. Soc.* **1989**, *111*, 4520. (b) Campisi, D.; Morii. T.; Barton, J. K. *Biochemistry* **1994**, *33*, 4130. (c) Pyle, A. M.; Morii, T., Barton, J. K. *J. Am. Chem. Soc.* **1990**, *112*, 9432. (d) Chow, C. S.; Behlen, E. S.; Uhlenbeck. O. C.; Barton, J. K. *Biochemistry* **1992**, *31*, 972.

(3) Sitlani, A.; Long, E. C.; Pyle, A. M.; Barton, J. K. *J. Am. Chem. Soc.* **1992**, *114*, 2303.

(4) David, S. D.; Barton, J. K. *J. Am. Chem. Soc.* **1993**, *115*, 2984.

(5) (a) Friedman, A. E.; Chambron, J.-C.; Sauvage, J.-P.; Turro, N. J.; Barton, J. K. *J. Am. Chem. Soc.* **1990**, *112*, 4960. (b) Jenkins, Y.; Friedman, A. E.; Turro, N. J.; Barton, J. K. *Biochemistry*, **1992**, *31*, 10809. (c) Hartshorn, R. M.; Barton, J. K. *J. Am. Chem. Soc.* **1992**, *114*, 5919.

(6) Krotz, A. H.; Kuo, L. Y.; Shields, T. P.; Barton. J. K. *J. Am. Chem. Soc.* **1993**, *115*, 3837.

(7) Sitlani, A.; Dupureur, C. M.; Barton, J. K. *J. Am. Chem. Soc.* **1993**, *115*, 12589.

(8) Kalsbeck, W. A.; Thorp, H. H. *J. Am. Chem. Soc.* **1993**, *115*, 7146.

(9) Pyle, A. M.; Rehmann, J. P.; Meshoyrer, R.; Kumar, C. V.; Turro, N. J.; Barton, J. K. *J. Am. Chem. Soc.* **1989**, *111*, 3051.

(10) Krotz, A. H.; Hudson, B. P.; Barton, J. K. *J. Am. Chem. Soc.* **1993**, *115*, 12577.

(11) Satyanarayana, S.; Dabrowiak, J. C.; Chaires, J. B. *Biochemistry* **1992**, *31*, 9319; **1993**, *32*, 2573.

(12) Eriksson, M.; Leijon, M.; Hiort, C.; Norden, B.; Graslund, A. *J. Am. Chem. Soc.* **1992**, *114*, 4933; **1994**, *33*, 5031.

(13) Haworth, I. S.; Elcock, A. H.; Freeman, J.; Rodger, A.; Richards, W. G. *J. Biol. Mol. Struct. Dyn.* **1991**, *9*, 23.

(14) Barton, J. K.; Goldberg, J. M.; Kumar, C. V.; Turro, N. J. *J. Am. Chem. Soc.* **1986**, *108*, 2081.

(15) (a) Rehmann, J. P.; Barton, J. K. *Biochemistry* **1990**, *29*, 1701. (b) Rehmann, J. P.; Barton, J. K. *Biochemistry* **1990**, *29*, 1710.

(16) (a) Baker, A. D.; Morgan, R. J.; Strekas, T. C. *J. Am. Chem. Soc.* **1991**, *113*, 1411. (b) Morgan, R. J.; Chatterjee, S.; Baker, A. D.; Strekas, T. C. *Inorg. Chem.* **1991**, *30*, 2687.

0002-7863/94/1516-9840$04.50/0

9,10-phenanthrenequinone diimine) in the hexanucleotide d(GTCGAC)$_2$ through partial insertion of the phi ligand at the central 5′-CG-3′ step.[4] In the 1:1 Δ-Rh(phen)$_2$phi^{3+}–d(GTCGAC)$_2$ complex, a specific loss of the internucleotide NOE was observed at the binding site of the rhodium complex (between C3 and G4), consistent with an intercalative model. Since Rh(phen)$_2$phi^{3+} promotes DNA cleavage upon photoactivation,[3] a photocleavage experiment could be used to correlate the site specificity of the complex with the selective internucleotide NOE loss. The sequence selectivity of the complex for 5′-pyrimidine-pyrimidine-purine-3′ steps (intercalating between the second pyrimidine and the purine), which are open in the major groove, is considered to be based upon shape-selection.[2,3] Several intermolecular NOEs between the metal complex and DNA also pointed to binding of the rigid complex from the major groove of the helix.[4] This result was again consistent with earlier photocleavage analysis which indicated that photocleavage of DNA by phi complexes of Rh(III) may proceed via specific abstraction of the H3′ hydrogen atom on the sugar to the 5′-side of the intercalation site;[3] this hydrogen is expected to point toward the major groove in an intercalated base step.

Here we present NMR evidence that intercalative binding from the major groove is apparent at a different DNA sequence with a phi complex of rhodium(III) containing different ancillary ligands. Photocleavage experiments on DNA restriction fragments had indicated a sequence-selectivity for $Rh(NH_3)_4$phi^{3+} favoring 5′-GC-3′ base steps.[6] Here NMR results are observed which are consistent with the binding of $Rh(NH_3)_4$phi^{3+} to d(TGGCCA)$_2$ via complete intercalation of the bidentate aromatic phi ligand and a sequence specificity which arises not through shape-selective steric interactions but through stabilizing hydrogen bonding from the ancillary ammine ligands to DNA. The NMR results point to a classical intercalative conformational change in the DNA, involving the full separation of the DNA base pairs to accommodate stacking by the complex from the major groove. Therefore a classical[17] intercalative model appears likely to be applicable in the design of what may be considered "nonclassical" synthetic, octahedral metallointercalators.

Experimental Section

Materials. [Rh(NH$_3$)$_4$phi]Cl$_3$, [Rh(cyclen)phi]Cl$_3$, and [Rh(S$_4$-cyclen)phi]Cl$_3$ were synthesized as previously described,[18,19] and concentrations were quantitated by UV-visible spectroscopy. The self-complementary deoxyoligonucleotide d(TGGCCA)$_2$ was synthesized on an ABI Model 392 DNA synthesizer using phosphoramidite chemistry, purified by established protocols, and quantitated using an extinction coefficient of 6,600 M^{-1} cm^{-1} per nucleotide at 260 nm.[20]

Instrumentation. UV–visible spectra were measured either on a Hewlett Packard 8452A diode array spectrophotometer or a Cary 2200 spectrometer. High performance liquid chromatography (HPLC) was performed with a Waters 600/600E multi solvent delivery system equipped with a Waters 484 tunable wavelength detector and a VYDAC protein & peptide C18 column. FPLC was performed on a Pharmacia FPLC system equipped with a LCC-500 plus controller, an LKB 2141 variable wavelength detector, and a PepRC 15 uM HR 16/10 (C18) column.

NMR Experiments. NMR spectra were obtained in 99.96% D_2O (Cambridge Scientific), and all samples were in phosphate buffer (10 mM $NaHPO_4$ / Na_2PO_4, 20 mM NaCl, pH 7.0). DNA samples were dissolved in 0.5 mL of phosphate buffer, repeatedly lyophilized from 99.8% D_2O, and then finally resuspended in 99.96% D_2O. Aliquots of a stock solution of $Rh(NH_3)_4$phi^{3+} were titrated directly into the NMR tube.

^{1}H-NMR spectra were recorded on a Bruker AMX-500 spectrometer operating at 500 MHz. The chemical shifts are referenced to the HDO resonance which was calibrated with sodium 3-(trimethylsilyl)-1-propanesulfonate at the corresponding temperature. The two dimensional (2-D) ^{1}H-COSY and NOESY experiments were acquired in the phase-sensitive mode using the time proportional phase incrementation method.[21] The spectra were recorded with the carrier frequency placed on the HDO resonance using 2048 points in t2 for 256–512 t1 values and a pulse repetition rate of 1.6 s. NOESY spectra were acquired for mixing times values of 200 and 300 ms. A presaturation pulse was utilized to suppress the HDO resonance. The data was apodized with a shifted sine bell or a squared sine bell, zero filled twice in t1, and Fourier transformed in both dimensions. One-dimensional (1D) and 2D-NMR spectra were processed using Bruker software.

Photocleavage Studies. For photocleavage studies, oligonucleotides were 5′-^{32}P-labeled with γ-ATP (DuPont) and T4 polynucleotide kinase (Boehringer Mannheim).[20] Reactions were loaded onto Nensorb-20 nucleic acid purification cartridges which were eluted with buffer A (100 mM Tris, 10 mM TEA, 1 mM EDTA), followed by 50:50 methanol/H_2O to remove 5′-^{32}P-labeled oligonucleotide. After lyophilization, 5′-^{32}P-oligonucleotides were used without further purification. Radioactivity was quantitated by Cherenkov counting with a Beckman LS500TD scintillation counter. Photocleavage reactions were irradiated at 325 nm for 5 min with a Liconix He/Cd laser (8 mW). Samples were loaded onto 20% denaturing polyacrylamide gels and eluted at 1600–2000 V for 1.5–2.0 h. Following electrophoresis, gels were wrapped and exposed to phosphoimager plates for 12–18 h. Phosphoimager plates were developed on a Molecular Dynamics Phosphoimager and images were processed using ImageQuant software. Gels were also exposed to film at −70 °C and developed with a Kodak X-OMAT processor.

Molecular Modeling. Molecular modeling was performed on a Silicon Graphics Iris Indigo Workstation using the Biosym modeling package (Biosym Technologies, San Diego, CA). A distance dependent dielectric ($\epsilon = 4R_{ij}$) and partially neutralized phosphates were employed in order more accurately to estimate the electrostatic energy term.[22] The overall 3+ charge of the rhodium complex was spread among the rhodium center and the ligands. AM1 calculations were used to calculate the partial charges on each atom of the neutral and protonated forms of ligands, and these were used to estimate[13] the partial atomic charges in the $Rh(NH_3)_4$-phi^{3+} complex.

Initial models of d(TGGCCA)$_2$ were constructed using Insight, and the crystal structure of a dinucleotide intercalation site.[23] The DNA structures were minimized for 100 steps with a steepest descents algorithm before placing the $Rh(NH_3)_4$phi^{3+} into the intercalation step. The coordinates of $Rh(NH_3)_4$phi^{3+} were taken from its crystal structure.[19] The starting models of $Rh(NH_3)_4$phi^{3+}–d(TGGCCA)$_2$ were minimized using Discover. During minimizations, the coordinates of the rhodium complex were fixed, but the ammine ligands were allowed to rotate about the Rh–N bonds. The C1′ and N1/N9 atoms of both T_1 and A_6 bases were also fixed to avoid fraying of the DNA. Hydrogen bonds between the base pairs were included as distance constraints using 50 kcal/mol/Å^2, and a force constant of 50 kcal/mol/Å^2 was employed for experimentally observed NOE contacts. The $Rh(NH_3)_4$phi^{3+}–d(TGGCCA)$_2$ complex was minimized for 100 steps using a steepest gradients algorithm, followed by 2000 steps with a conjugate gradients algorithm. A model was considered to be minimized when the maximum derivative was below 0.1 kcal mol^{-1} Å^{-1}.

Results and Discussion

^{1}H-NMR of d(TGGCCA)$_2$. The resonances of the free hexanucleotide were assigned primarily from NOESY spectra according to established methods.[24,25] In the NOESY spectrum of a right-handed duplex, each base H8 and H6 proton should exhibit an NOE cross peak to its own sugar H1′, H2′, and H2″

(17) Lerman, L. S. *J. Mol. Biol.* **1961**, *3*, 18.
(18) Pyle, A. M.; Chiang, M.; Barton, J. K. *Inorg. Chem.* **1990**, *29*, 4487.
(19) Krotz, A. H.; Kuo, L. Y.; Barton, J. K. *Inorg. Chem.* **1993**, *33*, 1940.
(20) Maniatis, T.; Fritsch, E. F.; Sambrook, J. *Molecular Cloning*: Cold Spring Harbor Laboratory, 1982.
(21) Marion, D.; Wuthrich, K. *Biochem Biophys. Res. Comm.* **1983**, *113*, 967.
(22) (a) Veal, J. W.; Wilson, W. D. *J. Biomol. Struct. Dynamics* **1991**, *8*, 1119. (b) Weiner, S. J.; Kollman, P. A.; Nguyen, D. T.; Case, P. A., *J. Comput. Chem.* **1986**, *7*, 230. (c) Weiner, S. J.; Kollman, P. A., Case, D. A.; Singh, U. C.; Ghio, C.; Alagana, G.; Piotete, S.; Weiner, P. *J. Am. Chem. Soc.* **1984**, *106*, 765.
(23) Wang, A. H. J.; Nathans, J.; van der Marel, G.; van Boom, J. H.; Rich A. *Nature* **1978** *276*, 471.
(24) Wuthrich, K. *NMR of Proteins and Nucleic Acids*; Wiley; New York, 1986.
(25) (a) Patel, D. J.; Shapiro, L.; Hare, D. *J. Biol. Chem.* **1986**, *261*, 1223. (b) Patel, D. J.; Shapiro, L. *J. Biol. Chem.* **1986**, *261*, 1230. (c) Patel, D. J., Shapiro, L. *Biopolymers* **1986**, *25*, 707. (d) Liu, X. L.; Chen, H.; Patel, D. J. *J. Biomolecular NMR* **1991**, *1*, 323.

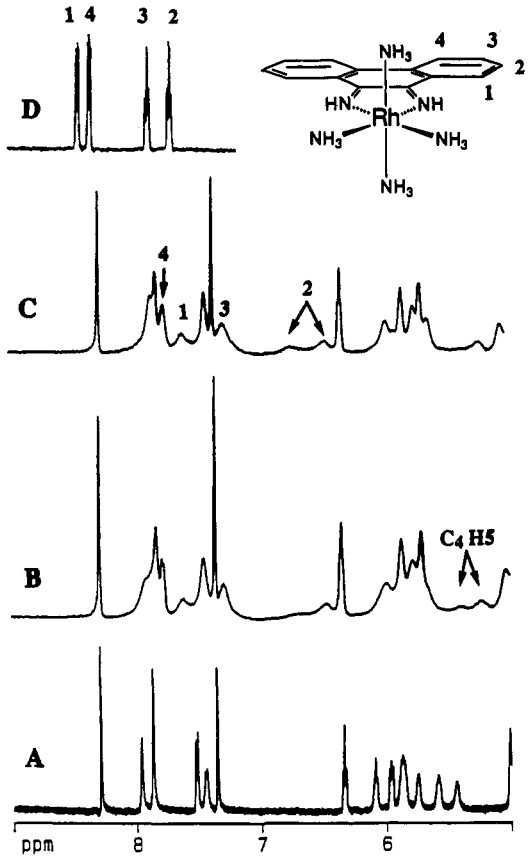

Figure 1. 500 MHz ^{1}H NMR spectrum of $Rh(NH_3)_4phi^{3+}$-$d(TGGCCA)_2$ at a ratio of metal to duplex of (A) 0, (B) 0.65, and (C) 0.90, in 10 mM phosphate, pH 7, containing 20 mM NaCl at 296 K. The ^{1}H NMR spectrum of free $Rh(NH_3)_4phi^{3+}$ under identical solution conditions is also shown (D) and the resonance assignments of the phi protons are given: 1, (1,8); 2, (2,7); 3, (3,6); and 4, (4,5).

protons as well as to the H1′, H2′, and H2″ protons on the flanking 5′ nucleotide residue. In the NOESY spectrum of the d(TGGCCA)$_2$, an NOE is observed from each base H8 and H6 resonances to its own sugar H2′/H2″ protons as well as to H2′/H2″ protons of the sugar of the nucleotide residue in the 5′ direction. Furthermore, in a standard B-form DNA duplex, the distance between the base H8/H6 proton to its own H2′ is approximately 2 Å and approximately 4 Å to the H2′ proton on the flanking 5′ sugar. For an A-form helix the opposite is found, with the shorter distance being to the H2′ proton of the 5′ sugar.[24,25] Since the NOE cross peak from each base H8/H6 proton to its own H2′ proton is larger than the cross peak to the H2′ proton on the 5′ sugar, it is concluded that the free hexanucleotide d(TGGCCA)$_2$ adopts a B-type conformation in solution.

^{1}H-NMR Titration of d(TGGCCA)$_2$ with $Rh(NH_3)_4phi^{3+}$. Figure 1 shows the ^{1}H-NMR titration of the hexanucleotide d(TGGCCA)$_2$ with $Rh(NH_3)_4phi^{3+}$. The base H8 and H6 resonances of the central 5′-GGCC-3′ region of the oligonucleotide exhibit small chemical shift movements and preferential broadening upon addition of $Rh(NH_3)_4phi^{3+}$. The significant broadening of these base resonances indicates that the exchange rate between the free and bound forms of the hexanucleotide is intermediate on the NMR time scale. This broadening is common with classical DNA intercalators, which generally bind to DNA with intermediate exchange kinetics.[26] In the case of the C_4H5 protons, however, where the chemical shift movement induced by the $Rh(NH_3)_4phi^{3+}$ is relatively large (approximately 0.17 ppm), separate resonances for the free and bound forms are observed. In the low ionic strength medium (20 mM NaCl) used to accumulate the spectra in Figure 1, the ratio of the bound:free form of the C_4H5 appears to be stoichiometric with the fraction of added $Rh(NH_3)_4phi^{3+}$. At higher NaCl concentrations (300 mM), however, the bound:free ratio of the C_4H5 resonance is somewhat less than the fraction of added metal complex. These results suggest that at low ionic strength there is a single predominant $Rh(NH_3)_4phi^{3+}$ binding site. As the ionic strength increases, other binding sites are also favored.

The assignment of the phi protons in the $Rh(NH_3)_4phi^{3+}$–d(TGGCCA)$_2$ complex was established from the NOESY spectrum of the 1:1 complex and by analysis of the one-dimensional spectrum as a function of temperature (increasing the temperature above the melting temperature of the 1:1 complex). Consistent empirically with intercalation,[26] it is observed, as illustrated in Figure 1, that the phi proton resonances move significantly upfield upon binding to d(TGGCCA)$_2$: (1,8), 0.84 ppm; (2,7), 1.01 and 1.26 ppm; (3,6), 0.60 ppm; and (4,5), 0.59 ppm.

The orientation of the phi ligand in the intercalation pocket may be estimated based upon intermolecular shielding values by examining the upfield movements of the phi resonances.[27] The upfield chemical shift movements of the phi resonances are consistent with all phi protons being positioned within the base stack. However, the chemical shift movements of the (2,7) and (1,8) proton resonances are significantly larger than those of the (3,6) and (4,5) protons. This difference in shift suggests that the (2,7) and (1,8) protons are located more toward the center of the base stack, where the ring current effects are most substantial, in comparison to the (3,6) and (4,5) protons. The particularly large upfield movement of the (2,7) protons suggests that these protons are located near, but in a plane above or below, the center of the G_3 residue. Necessarily, the (3,6) and (4,5) phi protons are placed more toward the edge of the GC base pair. These shifts therefore suggest that the rhodium complex intercalates so as to separate both sides of the base pair step rather than opening the base pairs in a wedge-like fashion.[11] It should be noted that the interpretation of these shift variations is simplified in comparison to other octahedral metal complexes which contain aromatic ancillary ligands, such as Δ-$Rh(phen)_2phi^{3+}$ [4] or Δ-$Ru(phen)_3^{2+}$,[15] since with the tetraammine complex, no ancillary ring currents are generated.

Although the phi (1,8), (3,6), and (4,5) pairs of protons yield only a single resonance, the phi (2,7) protons in the bound complex give rise to separate resonances, at 6.43 and 6.68 ppm. One explanation is that the two resonances represent the phi (2,7) protons bound at two distinct binding sites. This possibility is discounted as both resonances have the same integral, even though the downfield peak is broader. Also the ratio of the bound to free form of the C_4H5 resonance indicates that at low ionic strength $Rh(NH_3)_4phi^{3+}$ binds to d(TGGCCA)$_2$ predominantly at one site. A more likely explanation for the separate resonances is that $Rh(NH_3)_4phi^{3+}$ binds in an asymmetric fashion within the intercalation pocket, thereby removing the twofold symmetry of the phi ligand protons in free $Rh(NH_3)_4phi^{3+}$. This asymmetry may indicate canting of the metal complex in the site toward one strand, an aspect of binding indicated by photocleavage studies with other phi complexes of Rh(III).[3]

From the chemical shift difference of the inequivalent phi (2,7) resonances (determined at 285 K) the exchange rate, that is the effective dissociation rate, can be estimated at the temperature at which the two resonances coalesce. The exchange rate was determined to be 250 s^{-1} at the coalescence temperature of 305 K. The temperature at which coalescence occurs is somewhat lower than would be expected as the rate constant and difference in chemical shift will also be affected by the changing dynamics

(26) (a) Feigon, J.; Denny. W. A..; Leupin, W.; Kearns, D. R. *J. Med. Chem.* **1984**, 450. (b) Patel, D. J.; Canuel, L. L. *Biopolymers* **1977**, *16*, 857. (c) Patel, D. J.; Shen, C. *Proc. Natl. Acad. Sci. U.S.A.* **1978**, *75*, 2553. (d) Wilson, W. D.; Krishnamoorthy, C. R.; Wang, Y. H.; Smith, J. C. *Biopolymers* **1985**, *24*, 1941. (e) Chandrasekaran, S.; Jones. R. L.; Wilson, W. D. *Biopolymers* **1985**, *24*, 1941. (f) Delbarre, A.; Gourevitch, M. I.; Gaugain, B.; Le Pecq, J. B.; Roques, B. P. *Nucl. Acids Res.* **1983**, *11*, 4467.

(27) Giessner-Prettre, C.; Pullman, B. *Biochem. Biophys. Res. Commun.* **1976**, *70*, 578.

of the oligonucleotide as the temperature is increased. The exchange rate may also be estimated (although less accurately) directly from the difference in the chemical shift of the inequivalent phi (2,7) resonances at 285 K. At this temperature the line width of these resonances approach that of A_6H8, a resonance that shows little broadening upon addition of $Rh(NH_3)_4phi^{3+}$. The condition of slow exchange requires that the exchange rate be considerably less than the 112 Hz difference in chemical shift of the inequivalent phi (2,7) resonances. This suggests that the exchange rate is of the order of 10 s^{-1} at 285 K, which places the $Rh(NH_3)_4phi^{3+}$ complex between intermediate and slow exchange, a regime which is characteristic of many classical organic intercalators.[26,28,29]

Two Dimensional NMR Studies of 1:1 $Rh(NH_3)_4phi^{3+}$–d-$(TGGCCA)_2$. NOESY spectra were accumulated in order to obtain more structural information concerning the nature of $Rh(NH_3)_4phi^{3+}$ binding to $d(TGGCCA)_2$. In a NOESY spectrum of free $d(TGGCCA)_2$, an NOE is observed from each base H8 and H6 resonance to its own sugar H2′/H2″ protons as well as to the H2′/H2″ protons of the sugar of the nucleotide residue in the 5′ direction; this observation is typically seen in primarily B-form duplexes.[24,25] In the 300 ms NOESY spectrum of the 1:1 $Rh(NH_3)_4phi^{3+}$–$d(TGGCCA)_2$ complex shown in Figure 2, however, there is a complete absence of an NOE cross peak between the C_4H6 and the $G_3H2'/2''$ protons. The long mixing time used in this experiment should allow relatively strong buildup of NOE intensity (either via direct interaction or spin diffusion) from the C_4H6 to the $G_3H2'/H2''$ protons if the distance between the C_4 and G_3 base protons in the 1:1 $Rh(NH_3)_4phi^{3+}$–$d(TGGCCA)_2$ complex is less than 5 Å. It is noteworthy that in the free hexamer without bound metal complex this NOE is clearly observed and relatively strong in intensity. This selective NOE loss therefore indicates that the distance between these protons has significantly increased upon binding of the $Rh(NH_3)_4phi^{3+}$. Importantly, coincident with this loss of connectivity in the $Rh(NH_3)_4phi^{3+}$–$d(TGGCCA)_2$ complex, new NOE peaks are observed between phi protons and protons from the G_3 and C_4 deoxyribose sugars.[30] There are also similar but less clearly defined losses in internucleotide NOE connectivities evident between the aromatic H8/H6 base protons and sugar H1′ protons. Therefore the loss of the sequential internucleotide NOE connectivity, coupled with the presence of NOE cross peaks between phi protons and protons from the G_3 and C_4 sugar residues indicates sequence-specific intercalation between the G_3 and C4 bases. NOESY spectra of the 1:1 complex were also accumulated at 296, 305, and 310 K. Similar results were obtained in all cases.

Overall, few NOE cross peaks between $Rh(NH_3)_4phi^{3+}$ and $d(TGGCCA)_2$ are observed, however, even at long mixing times. Not many intermolecular NOEs are expected, since the exchange of the ancillary ammine protons precludes the observation of intermolecular NOEs between the ancillary ligands and DNA. The strongest intermolecular NOE cross peak observed is between the phi (1,8) protons to the C_4H2' proton in the major groove. The observed cross peak between the phi (1,8) and the minor groove C_4H2'' is also relatively strong in the NOESY with 300 ms mixing time; however, comparison of the relative intensities of these cross peaks in a 200 ms mixing time NOESY spectrum indicates that at 300 ms the cross peak from the phi (1,8) to the minor groove C_4H2'' is largely due to spin diffusion. Another set of diagnostic NOE cross peaks are observed between phi (3,6) and G_3 H2′2″ protons, and this is the only cross peak seen between the phi (3,6) protons and DNA. Finally, additional NOEs are observed between the phi (1,8) and phi (2,7) protons and G_3-H2′/2″; both of these sets of cross peaks are weaker than the phi (3,6) - G3H2′2″ NOEs at all mixing times. Taken in combination and given the rigidity of the $Rh(NH_3)_4phi^{3+}$ complex, the NOE cross peaks can only be explained by *intercalation from the major groove*, and it is therefore concluded that $Rh(NH_3)_4phi^{3+}$ is binding the DNA duplex from the major groove.

Binding to the DNA duplex in the major groove is uncommon in the case of small molecules[28,29] although typical with larger DNA-binding proteins.[31] Nonetheless, it may be generally the case that access from the major groove is a feature of binding by metallointercalators. Evidence for a major groove orientation with intercalation has been obtained for Pt(terpy)HET$^+$ (HET = 2–hydroxyethanethiolate),[23] $Rh(phen)_2phi^{3+}$, and $Rh(phi)_2$-bpy^{3+},[3,4] as well as $Ru(phen)_3^{2+}$.[14,15,32]

The crystal structures[23,28,29,33] of several intercalators in dinucleotides have revealed a differential sugar puckering, C3′-endo puckering to the 5′-side of the intercalation site and C2′-endo puckering to the 3′-side, and in early studies, this alternation in sugar pucker was used to explain the neighbor excluded binding to DNA of simple flat intercalators which lack sequence specificity.[34,35] We sought to examine whether with the sequence-selective $Rh(NH_3)_4phi^{3+}$ any alternation in sugar puckering could be established using NMR.[36] The 2D-NOESY spectrum of free $d(TGGCCA)_2$ certainly supports a B-DNA conformation for the hexamer, characterized by C2′-endo sugar pucker. We examined the 2D-COSY spectra of the 1:1 complex, since $^3J_{HH}$ coupling may also be used to estimate the position of the equilibrium between the C_2'-endo and C_3'-endo conformations of the deoxyribose sugar ring.[24] Assessments of $^3J_{HH}$ couplings in the 1:1 complex consistently establish that the C_4 sugar, to the 3′-side of the intercalation site, adopts the C2′-endo conformation. Owing to the overlap and broadening of G_3 with G_2 sugar protons, however, no firm conclusion could be drawn specifically regarding the puckering in the G_3 sugar.

Photocleavage of $d(TGGCCA)_2$ by $Rh(NH_3)_4phi^{3+}$. Photocleavage studies were conducted to verify the binding of $Rh(NH_3)_4phi^{3+}$ to the central 5′-G_3C_4-3′ step of the oligonucleotide. This conclusion, based on the broadening of resonances in the 1D-NMR spectra, the selective loss in internucleotide NOE intensity, and the presence of specific intermolecular NOEs, is further supported by the DNA cleavage experiments. Upon photoactivation, cleavage by $Rh(NH_3)_4phi^{3+}$ is observed predominantly at G_3 (Figure 3). This cleavage is fully consistent with earlier studies on long DNA restriction fragments where $Rh(NH_3)_4phi^{3+}$ is found to target 5′-GC-3′ base steps.[6]

It is noteworthy that with the tetrammine complex, as with other phi complexes of rhodium which contain saturated amines in the ancillary position,[6] we observe cleavage to some extent at positions both to the 3′- as well as 5′-side of the intercalation site. In the case of the hexamer we have also detected cleavage at C_4 but to a lesser extent. The more intense cleavage, nonetheless, is to the 5′-side, here at G_3. This cleavage pattern, seen consistently on longer DNA restriction fragments, shows a 5′-asymmetry in intensity, consistent with association from the major groove.[37] It is interesting to compare this pattern of cleavage, however, to that of $Rh(phen)_2phi^{3+}$, which promotes highly 5′-asymmetric cleavage patterns with essentially no cleavage in the 3′-position.

(28) Berman, H. M.; Young, P. R. *Ann. Rev. Biophys. Bioeng.* **1981** *10*, 87.

(29) Neidle, S.; Abraham, Z. *CRC Crit. Rev. Biochem.* **1984**, *17*, 73.

(30) Although the G_2 and G_3 H2′ and H2″ resonances overlap, the NOE crosspeaks B and C in Figure 2 may be assigned to the G_3 sugar protons given the selective loss of the NOE crosspeak between the C_4H6 and the G_3 H2′/H2″ protons.

(31) Pabo, C. O.; Sauer, R. J. *Ann. Rev. Biochem.* **1992**, *61* 1053.

(32) Based on NMR and luminescence experiments, we have proposed that $Ru(phen)_3^{2+}$ binds DNA with low overall affinity through two primary modes, partial intercalation in the major groove and hydrophobic binding against the surface of the minor groove.

(33) Aggarwal, A.; Islam, S. A.; Kuroda, R.; Neidle, S. *Biopolymers* **1984**, *23*, 1025–1041.

(34) Bond, P. J.; Langridge, R.; Jennette, K. W.; Lippard, S. J. *Proc. Natl. Acad. Sci. U.S.A.* **1975**, *72*, 4825.

(35) Sobell, H. M.; Tsai, C. C.; Jain, S. C.; Gilbert, S. G. *J. Mol. Biol.* **1977**, *114*, 333.

(36) Since organic intercalators such as ethidium and proflavine lack sequence-specificity, 2D-NMR techniques cannot be used to establish an alteration in sugar puckering on intercalation.

(37) Sluka, J. P.; Horvath, S. J.; Bruist, M. F.; Simon, M. I.; Dervan, P. B. *Science* **1987**, *238*, 1129.

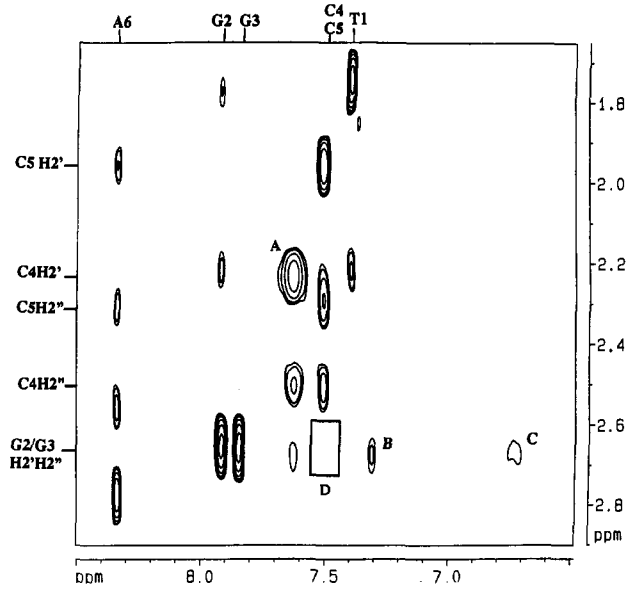

Figure 2. Expansion of a 300 ms mixing time NOESY at 310 K of the 1:1 $Rh(NH_3)_4phi^{3+}$–$d(TGGCCA)_2$ complex (1.3 mM in 10 mM phosphate, pH 7, containing 20 mM NaCl) showing the connectivities between the oligonucleotide base H8/H6 and phi protons (8.5–6.5 ppm) to the sugar H2′/H2″ protons (2.9–1.7 ppm). Intermolecular cross peaks are also evident: (A) phi (1,8) to C_4H2'; (B) phi (3,6) to $G_3H2'/H2''$; and (C) phi (2,7) to $G_3H2'/H2''$. The box denoted (D) indicates the position where an NOE cross peak between the C_4H6 and the $G_3H2'/H2''$ protons would appear if $Rh(NH_3)_4phi^{3+}$ bound without specific intercalation.

This different characteristic pattern of cleavage for the ammine complexes may reflect the deeper intercalation of the phi ligand in the intercalation pocket. From modeling, with the complex stacked deeply in the base pair column, the photoexcited phi ligand is well positioned to activate hydrogen abstraction on the sugar to the 3′-side of the intercalation step as well as to the 5′-side. It is interesting to consider the internucleotide NOE intensities in this context, where we find that the highest intensity NOEs in the 1:1 complex with $Rh(NH_3)_4phi^{3+}$ are those from the phi protons to the C2′-H of C_4, not G_3.

The site-selectivity of $Rh(NH_3)_4$ phi^{3+} differs from classical intercalators (e.g., ethidium, proflavine) which typically stack in 5′-pyrimidine-purine-3′ steps to maximize stacking interactions with the purine bases.[28,29] The sequence selectivity of $Rh(NH_3)_4$ phi^{3+} also differs from that of Δ-$Rh(phen)_2phi^{3+}$, which selectively targets 5′-pyrimidine-pyrimidine-purine-3′ sites (intercalating between the second pyrimidine and the purine base); the selectivity of Δ-$Rh(phen)_2phi^{3+}$ likely arises from steric clashes of the ancillary phenanthroline protons and the DNA bases at sites which are not opened in the major groove.[2] In the case of $Ru(phen)_3^{2+}$, where singlet oxygen mediated photocleavage experiments have been conducted, no site selectivity in binding has been observed.[38] We attribute the site-selectivity of $Rh(NH_3)_4$ phi^{3+} to hydrogen bonding by the ancillary ammines to the guanine O6 atoms above and below the intercalation site. This 5′-GC-3′ selectivity has been observed also with Rh(cyclen)phi^{3+} and $Rh(en)_2phi^{3+}$, all capable of donating an axial amine for hydrogen bonding, but not with $Rh(S_4$-cyclen)phi^{3+} or $Rh(phen)_2phi^{3+}$, which cannot donate hydrogen bonds from ancillary ligands.[6] Shown in Figure 3 is also cleavage on the hexamer by Rh(cyclen)-phi^{3+} at G_3, while $Rh(S_4$-cyclen)phi^{3+} is seen to cleave primarily at C_4.

Molecular Modeling of the $Rh(NH_3)_4phi^{3+}$–$d(TGGCCA)_2$ Complex. The photocleavage and 2D-NOESY experiments demonstrate that $Rh(NH_3)_4phi^{3+}$ intercalates into the hexanucleotide $d(TGGCCA)_2$ from the major groove between the G_3 and C_4 residues. Due to the relatively long mixing times needed to observe the intermolecular NOE cross peaks and because of the few intermolecular NOEs available, it is not possible to obtain a detailed quantitative model of the $Rh(NH_3)_4phi^{3+}$–$d(TGGCCA)_2$ complex. We may, however, explore models for $Rh(NH_3)_4phi^{3+}$ intercalated into the DNA helix in the context of the NMR data presented here and the biochemical data[6] previously presented.

Initial models were constructed based upon criteria from several experiments. The 2D-NOESY spectra described here indicate intercalation of $Rh(NH_3)_4phi^{3+}$ in the hexamer from the major groove with insertion of the phi ligand into the central G3-C4 base step. The observed intermolecular NOEs provided conservative constraints of ≤5.5 Å for the ten pairs of protons (without ordering). The lack of nonexchangeable protons on the ancillary ligands of $Rh(NH_3)_4phi^{3+}$ preclude the observation of intermolecular NOEs between the ancillary ligands and DNA in D_2O. Based upon plasmid DNA unwinding experiments,[6] an unwinding angle of 20° per rhodium complex bound may be used in the starting models. It is noteworthy that in the molecular mechanics calculation, only small perturbations from this initial unwinding would be expected. The 2D-COSY experiments on the 1:1 complex indicate that the C_4 sugar adopts the C2′-endo conformation, but no conclusion could be drawn with respect to the conformation of the G_3 sugar. Therefore, initial models with both C_2'-endo and C_3'-endo sugar puckering at G_3 were constructed; we cannot experimentally distinguish between them. For simplicity, these will be referred to as the C3′-endo and C2′-endo models. We have also considered all other sugar residues as adopting the C2′-conformation, based upon the NMR data for the free duplex. For the C2′-endo model of the intercalation site, $d(TGGCCA)_2$ was built using Insight II as a B-DNA duplex, except that a 6.76 Å rise and a −16° twist (i.e., 20° unwound) parameters were specified at the G_3-C_4 intercalation step. For the C3′-endo model of $d(TGGCCA)_2$, the coordinates at the G_3-C_4 intercalation step were taken from the crystal structure of $d(CG)_2$ with Pt(terpy)HET^+.[23] A range of starting structures were examined with both DNA models (C2′-endo or C3′-endo). The rhodium complex was placed close to each strand, tilted in the site, intercalated deeply in the pocket as well as being positioned at the entry of the site.

Figure 4 shows the lowest energy structure with a C3′-endo starting model. The intermolecular NOE constraints imposed are satisfied by this model. Variations in the initial orientation of the metal complex in the site produced negligible differences in the final structure of lowest energy. The general features of the lowest energy structure with a C2′-endo starting model are also quite similar, despite the difference in sugar puckering; our experimental constraints are insufficient to warrant the determination of the sugar conformation. As illustrated in Figure 4, in all of the models, the phi ligand is seen to stack with the purine bases in the intercalation site. The pyrimidine bases become propeller twisted away from their initial idealized coplanar orientations, but the purine residues remain parallel to the phi ligand, maximizing stacking overlap between the purine and phi. This result is interesting in light of the noted preference of classical intercalators for 5′-pyrimidine-purine-3′ steps, a sequence preference considered to maximize purine-intercalator stacking interactions.[28,29]

The models are also consistent with the upfield chemical shifts seen in the phi aromatic protons on binding to the hexamer. In both C2′-endo and C3′-endo models, the phi (1,8) and (2,7) protons are positioned more directly under the base pairs than the (3,6) and (4,5) protons, and the leading edge of the phi ligand extends into the minor groove of the central GC base step. The phi (1,8) and (2,7) protons are stacked between the cytosine aromatic ring and the five-membered ring of the guanosine aromatic base. Theoretical predictions[27] of the shielding effects of the aromatic bases suggests that placing a proton 3.4 Å above the centers of the aromatic rings should produce strong upfield shifts of the

(38) Mei, H. Y.; Barton, J. K. *Proc. Natl. Acad. Sci. U.S.A.* **1988**, *85*, 1339.

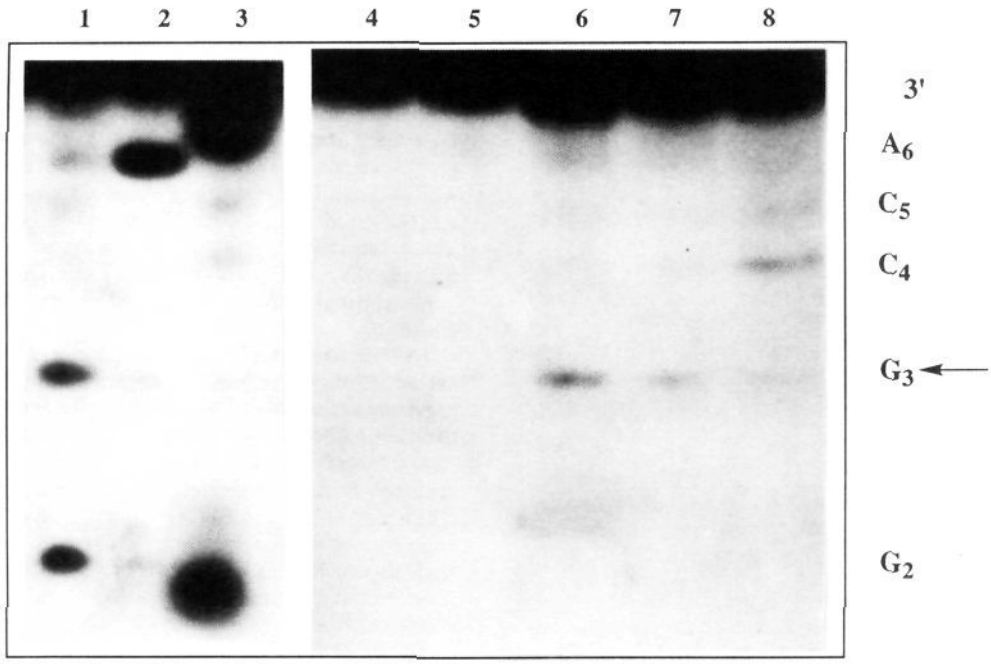

Figure 3. Autoradiogram of an 20% denaturing polyacrylamide gel after irradiation of 5′-[^{32}P]-labeled $d(TGGCCA)_2$ in the presence and absence of metallointercalators. Photocleavage conditions: 10 μM duplex DNA, 10 μM Rh, pH 7.0, 10 mM NaCacodylate, 40 mM NaCl, 5 min irradiation at 325 nm using a Liconix He/Cd laser (power = 8 mW). Lanes 1, 2, and 3 show Maxam-Gilbert G, A + G, and C + T sequencing reactions, respectively. Lane 4 is labeled DNA without treatment; lane 5, oligonucleotide irradiated in the absence of rhodium; lanes 6–8, irradiation in the presence of $Rh(NH_3)_4phi^{3+}$, $Rh([12]aneN_4)phi^{3+}$ and $Rh([12]aneS_4)phi^{3+}$, respectively. Note that the complexes which contain axial amines ($Rh(NH_3)_4phi^{3+}$ and $Rh([12]aneN_4)phi^{3+}$) cleave specifically at G_3, corresponding to intercalation in the central 5′-G_3C_4-3′ base step, while $Rh([12]aneS_4)phi^{3+}$, which lacks hydrogen bonding donors in the axial positions, cleaves at a different site on the oligonucleotide duplex.

order observed experimentally (about 1 ppm). Protons at the periphery of the aromatic bases, such as the phi (3,6) and (4,5) protons, would experience smaller upfield shifts.

Only slight asymmetry is apparent in the overall positioning of $Rh(NH_3)_4phi^{3+}$ within the intercalation site in both C2′-endo and C3′-endo models. It is not clear whether the small asymmetry evident is sufficient to account for the difference in shift between the phi (2) and (7) protons observed in the NMR spectra. However, other protons on the phi ligand are not found to be inequivalent in the bound form, and the phi (2, 7) positions are likely to be most sensitive to asymmetries in shielding given their large upfield shift in the 1:1 complex.

The model does, however, reflect the rationale for the sequence-selectivity of the tetraammine complex. As evident in Figure 4, the axial ammines of the rigid complex upon intercalation are well positioned for hydrogen bonding to the guanine O6 atoms. The hydrogen bonds in this model are characterized by a 2.9–3.0 Å N–O distance and a linear N–H–O alignment for both hydrogen bonds above and below the site of intercalation. Importantly, despite deep intercalative binding in the $Rh(NH_3)_4phi^{3+}$: $d(TGGCCA)_2$ complex, no steric clash is evident between the ancillary NH_3 ligands and the DNA helix. Instead, intercalation of the phi ligand brings the ancillary axial ammines into position for hydrogen bond donation.

Two minor groove orientations were also examined as starting structures. The minimum energy configurations obtained could not satisfy the conservative NOE constraints. Also the ordering of NOE intensities to the different phi protons (at both mixing times) was inconsistent with a minor groove orientation.

Although the NMR data do not allow for a detailed structure determination of $Rh(NH_3)_4phi^{3+}$ bound to $d(TGGCCA)_2$, the results do provide an adequate set of constraints in support of the general mode of binding by these complexes which has been proposed.[6] The complexes intercalate into the G_3-C_4 step through deep insertion of the aromatic phi ligand, and this intercalation is characterized by a complete separation of the G_3 and C_4 base pairs. The unstacking of the G_3 and C_4 base pairs may be compensated for energetically through the new stacking of guanine bases with the phi ligand. The intercalation of the phi ligand positions the axial ammine ligands to donate hydrogen bonds to the O6 positions of the guanine bases.

Comparison of NMR Studies on Different Metal Complexes Bound to Oligonucleotides. The presence of NMR data concerning the DNA binding of Δ-$Ru(phen)_3^{2+}$,[12,15] Δ-$Rh(phen)_2phi^{3+}$,[4] and now $Rh(NH_3)_4phi^{3+}$ allows for interesting and informative comparisons to be made among them. The chemical shift movements of the phenanthroline and phi resonances for Δ-$Ru(phen)_3^{2+}$, Δ-$Rh(phen)_2phi^{3+}$, and $Rh(NH_3)_4phi^{3+}$ on binding to oligonucleotides are given in Table 1. The resonances of the peripheral phenanthroline (4,7) and (5,6) protons of $Rh(phen)_2phi^{3+}$ show virtually no movement upon binding to DNA. In contrast, all the phi resonances of this complex and of $Rh(NH_3)_4phi^{3+}$ show significant upfield shifts as a result of selective intercalation of the phi ligand into the base stack. This pattern indicates that when a coordinated phenanthroline ligand is located in the DNA groove little or no chemical shift movement is expected for the phenanthroline (4,7) or (5,6) resonances. However, the phenanthroline (4,7) and (5,6) resonances of Δ-$Ru(phen)_3^{2+}$ do show significant upfield movement in chemical shift upon oligonucleotide binding. This upfield shift indicates that one of the ligands is not bound (at least totally) in the groove. Furthermore, because the binding of $Ru(phen)_3^{2+}$ to the oligonucleotide occurs with fast exchange on the NMR time scale, the upfield chemical shift movements observed for the phenanthroline protons represent the exchange-averaged movement of all three phenanthroline ligands. As only one ligand could intercalate at any given time, the upfield chemical shift changes of the phenanthroline (4,7) and (5,6) resonances may essentially be multiplied by a factor of 3 to obtain an effective upfield movement of these resonances for the one phenanthroline ligand that does not bind in the groove. On this basis, the upfield shifts shown by the phenanthroline resonances of Δ-$Ru(phen)_3^{2+}$ on binding to DNA are completely consistent with the chemical shift movements shown by the resonances of the phi ligands in Δ-$Rh(phen)_2phi^{3+}$ and $Rh(NH_3)_4phi^{3+}$, both of which bind by intercalation. For comparison, intercalated proton resonances

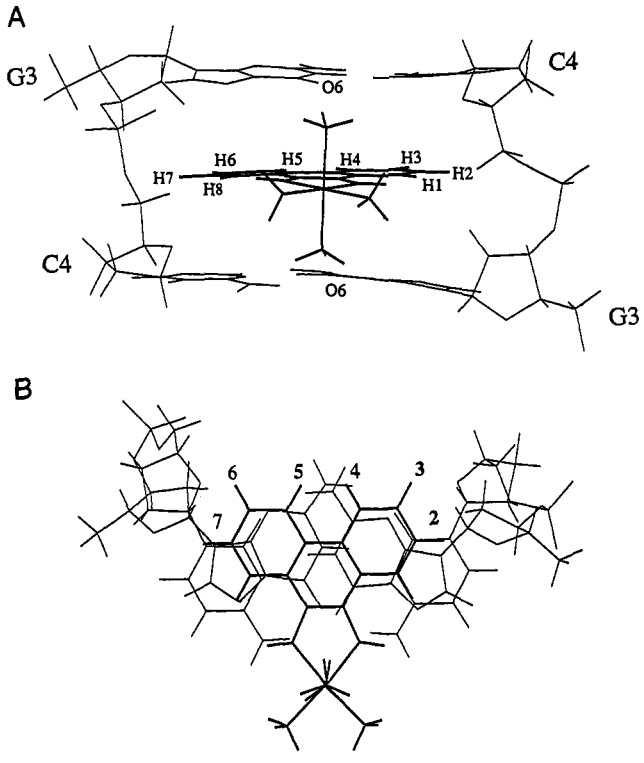

Figure 4. Views perpendicular to the helix axis (A) and down the helical axis (B) of an energy minimized model of $Rh(NH_3)_4phi^{3+}$ intercalated into the 5′-G_3C_4-3′ step of $d(TGGCCA)_2$. Shown is an energy-minimized model with alternation of the sugar-puckering in the intercalation step (C3′-endo model). The metal complex is shown in bold. $Rh(NH_3)_4phi^{3+}$ was manually docked into the G_3-C_4 step from the major groove, constrained with the observed NOE contacts, and minimized with the Discover program using a conjugate gradient algorithm. The relative upfield shifts of the aromatic phi protons on binding to the oligonucleotide can be understood in the context of the model, where the maximum upfield shift is seen for the phi (2,7) proton resonances. The selectivity of the metal complex for 5′-GC-3′ steps can also be understood based upon the hydrogen bonding evident in this model between the axial ammines of the complex and the guanine O6 atoms above and below the intercalation site.

Table 1. Upfield Chemical Shift Movements[a] in Metal Complexes upon Oligonucleotide[b] Binding

proton	Δ-$Ru(phen)_3^{2+}$ (ppm)	Δ-$Rh(phen)_2phi^{3+}$ (ppm)	$Rh(NH_3)_4phi^{3+}$ (ppm)
phen (2,9)	0.17	–0.18, 0.15	
phen (3,8)	0.16	–0.05, –0.18	
phen (4,7)	0.28	0.04, –0.02	
phen (5,6)	0.31	0.01	
phi (1,8)		0.58	0.84
phi (2,7)		0.83	1.10
phi (3,6)		0.88	0.60
phi (4,5)		0.73	0.59

[a] Data are taken for Δ-$Ru(phen)_3^{2+}$ and Δ-$Rh(phen)_2phi^{3+}$ from refs 15a and 4, respectively. Shown here as positive shift differences are those shifts which are upfield in the presence of DNA compared to shifts in the absence of DNA. [b] Data are reported for Δ-$Ru(phen)_3^{2+}$ bound to $d(GTGCAC)_2$ and Δ-$Rh(phen)_2phi^{3+}$ bound to $d(GTCGAC)_2$.

of ethidium bromide displays upfield shifts of 0.75 ppm on average.[26] With octahedral metallointercalators, as with classical organic intercalators, then, a substantial upfield chemical shift of protons on the aromatic ligand may be viewed as a signature of the intercalation of that ligand.

Interestingly, the pattern of upfield chemical shift movement for the three complexes likely reflects also the differences in their binding to DNA. Comparisons of absolute chemical shift changes for different ligand systems are difficult, but certainly parallels may be drawn with respect to relative shift movements for different resonances. With both Δ-$Ru(phen)_3^{2+}$ and Δ-$Rh(phen)_2phi^{3+}$, steric clashes of ancillary phenanthroline protons with the DNA bases should preclude a deep intercalation of the coordinated ligand, such as is observed with $Rh(NH_3)_4phi^{3+}$. Consistent with this notion, the largest chemical shift changes for Δ-$Ru(phen)_3^{2+}$ [15] and Δ-$Rh(phen)_2phi^{3+}$ [4] are seen in the peripheral phenanthroline (5,6) and phi (3,6) protons which are located at the leading edge of the intercalating ligand. In the case of $Rh(NH_3)_4phi^{3+}$, in contrast, the largest shifts of the intercalated phi are seen at the (2,7) positions, at the side of the intercalating ligand. $Rh(NH_3)_4phi^{3+}$ is positioned deeply in the intercalation pocket. This deeper stacking also permits a larger surface area for overlap with the DNA base pairs and hence likely a larger overall DNA binding affinity. At ambient temperature, the complexes Δ-$Ru(phen)_3^{2+}$, Δ-$Rh(phen)_2phi^{3+}$, and $Rh(NH_3)_4phi^{3+}$ bind to DNA hexamers with fast, intermediate, and intermediate-slow exchange, respectively; also their overall duplex DNA binding constants are estimated to be $\geq 10^3$, 10^6, and 10^6 M^{-1}, respectively.[2,6,14,15]

The 2D-NOESY data also may be understood based upon the different binding characteristics of these complexes. Both Δ-$Rh(phen)_2phi^{3+}$ and $Rh(NH_3)_4phi^{3+}$ bind to their oligonucleotide sites with high specificity.[3,6] Hence a sequential internucleotide NOE walk is expected to reveal a loss of NOE intensity selectively at the site of intercalation. Indeed, for $Rh(NH_3)_4phi^{3+}$, which binds with the slowest exchange kinetics of the three complexes, a complete loss of internucleotide NOE intensity is observed at the binding site; for Δ-$Rh(phen)_2phi^{3+}$, a loss in internucleotide NOE intensity is also observed.[4] For Δ-$Ru(phen)_3^{2+}$, the absence of this loss of NOE intensity has been taken as evidence against intercalation,[12] but with the fast exchange kinetics and lack of sequence specificity of $Ru(phen)_3^{2+}$, little reduction in internucleotide NOE intensity should be expected. It is also noteworthy that the 2D-NOESY data reveal intermolecular NOEs for $Ru(phen)_3^{2+}$ [12] and Δ-$Rh(phen)_2phi^{3+}$ [4] to AH2 protons in the minor groove; for $Rh(NH_3)_4phi^{3+}$ no direct NOEs (without spin diffusion) can be attributed to minor groove interaction. Importantly, the 2D-NOESY data for both Δ-$Rh(phen)_2phi^{3+}$ [4] and $Rh(NH_3)_4phi^{3+}$ bound to oligonucleotides indicate several intermolecular NOEs to major groove protons, and, in the presence of $Ru(phen)_3^{2+}$,[15] a substantial shift in the thymine methyl resonance is observed. These data are consistent with at least two binding modes for $Ru(phen)_3^{2+}$ and to some extent for Δ-$Rh(phen)_2phi^{3+}$ under these conditions of high concentration and low ionic strength; the phenanthroline ligands may promote hydrophobic association in the minor groove.[32] For $Rh(NH_3)_4phi^{3+}$, with its hydrogen bonding ammine ligands, no similar minor groove association is detected. Instead binding to the oligonucleotide by $Rh(NH_3)_4phi^{3+}$ in one mode, through intercalation in the major groove, is observed.

Conclusions. The results described here indicate that $Rh(NH_3)_4phi^{3+}$ binds to $d(TGGCCA)_2$ by sequence-selective intercalation in the major groove. Major groove access may be a general characteristic of metallointercalation. The octahedral complex binds to the duplex in a manner consistent with classical intercalation, with separation of the DNA base pairs to accommodate stacking. The site-selectivity of $Rh(NH_3)_4phi^{3+}$ depends upon hydrogen bonding contacts of the ancillary, nonintercalating ligands of the synthetic complex with the DNA bases. Although the general binding mode may, therefore, be regarded as classical, the metallointercalators themselves may be regarded as nonclassical, since their sequence-selectivity is derived from the nonintercalating functionalities of the octahedral complex. Structural studies with octahedral metallointercalators point to a general strategy for the design of sequence-specific DNA-binding molecules in the major groove.

Acknowledgment. We are grateful for the financial support of the National Institutes of Health (GM33309 to J.K.B. and an N.I.H. traineeship to T.P.S.) in this research. We also thank W. D. Wilson and R. J. Lombardy for force field parameters in the modeling studies.